Tunneling of laser-generated free electrons in semiconductor double wells

W. Pötz
Physics Department, University of Illinois at Chicago, Chicago, Illinois 60607

M. Žiger and P. Kocevar
Institut für Theoretische Physik, Universität Graz, A-8010 Graz, Austria
(Received 28 December 1994)

A theoretical study of the dynamics of free photogenerated carriers in resonance-biased asymmetric GaAs-$Al_xGa_{1-x}As$ double wells is presented. We consider a situation where photogeneration takes place on a subpicosecond time scale and, initially, produces a coherent ensemble of free electron-hole pairs in the wide well. The simultaneous thermalization and tunneling of electrons between the two wells is analyzed within the density matrix approach. The interplay between tunneling and Coulomb scattering is explored at several levels of approximation regarding free-carrier screening. We find that the Coulomb interaction represents an effective agent to destroy phase coherence and to damp out coherent charge oscillations in the system. Our calculations predict that, if the free-carrier Coulomb interaction provides the dominant dephasing mechanism in the system, coherent charge density oscillations associated with *free* carriers should persist up to electron sheet densities of about 3×10^{10} cm^{-2}. It is shown that, under present conditions, dynamic screening within the plasmon-pole approximation and static screening give virtually identical results.

I. INTRODUCTION

A variety of optical techniques, such as four-wave mixing and ultrafast pump-probe techniques, have been developed to monitor subpicosecond transport phenomena and thermalization of hot photogenerated carriers in semiconductors, including bulk materials, quantum-well heterostructures, and superlattices.[1,2] Radiation emitted by accelerated charges has given indirect evidence for the presence of Bloch oscillations in superlattices, as well as coherent charge oscillations in semiconductor double wells.[3–6] The latter have been reported for resonantly laser-generated excitons in asymmetric quantum wells, in which an applied electric field was used to tune electronic subband levels into resonance.[3,4] In their function as generators of electromagnetic radiation in the THz regime, asymmetric semiconductor double wells may be developed into useful nanostructure devices based on the quantum-interference principle.[7] We would also like to point out that in piezoelectric systems, *sound generation* in the same frequency range should be possible.

To our knowledge, only exciton-related coherent charge oscillations have been reported to date and no experimental evidence has been reported for the presence of coherent free-carrier oscillations in double wells. One may be tempted to give qualitative arguments why excitons display coherent oscillations more readily than free carriers. The exciton has a localized nature and any imperfections in the structure tend to detune affected exciton levels. Therefore, excitons are excited somewhat selectively, whereas free carriers are given different excess energies when created near structural imperfections. Moreover, carriers bound in excitons are less reactive than free carriers, leading to longer phase coherence times, at least for low exciton densities, where the exciton radius is small compared to the average exciton-exciton distance. Finally, excitons are generally easier to monitor than free carriers.[8] On the other hand, a careful analysis of modulations of the absorption coefficient has recently revealed evidence for free-carrier oscillations in biased bulk semiconductors.[9]

In the present work, we perform a theoretical investigation of the simultaneous generation, tunneling, and thermalization of photogenerated free electron-hole pairs in asymmetric double wells, addressing the question of whether the charge oscillations observed for excitons can also exist in the free-particle regime at higher excitation energies. Our study focuses on the interplay between the coherent process of tunneling between wells and dissipation provided by the Coulomb interaction. Details of the laser-excitation process of free carriers are not considered here.[10] Moreover, we consider experimental situations in which only the two lowest electron subband levels are at resonance, so that hole tunneling may be neglected.

A study of thermalization in a nonequilibrium Coulomb system necessarily leads to the notorious problem of screening of the interaction. In three-dimensional (3D) systems, it has been found that dynamic screening within the plasmon-pole approximation (PPA) leads to Coulomb scattering rates, which are significantly different (larger according to Ref. 11, smaller according to Ref. 12) from those obtained within static screening. For our study, it is imperative not to underestimate the effective strength of the Coulomb interaction. Therefore, we used and compared several versions of free-carrier screening, including dynamic screening within the PPA.

Our paper is organized as follows. The theoretical approach based on the density matrix approach is outlined in Sec. II A. The screening models that are used in the

0163-1829/95/52(3)/1959(11)/$06.00

present study are summarized in Sec. II B, with a more detailed discussion of the PPA added in the Appendix. Sec. III contains results of a numerical study of coherent charge oscillations in double wells and their dependence on excitation conditions, structure parameters, and the screening model employed. Summary and conclusions are given in Section IV.

II. THEORY

A. Density matrix approach

Our model is based on the density matrix approach.[13,14] It is well suited for situations where (quasi-)particle-particle interactions are weak to moderate and phase coherence plays an important role in the system. It represents a direct generalization of Boltzmann transport theory into the quantum regime and combines the virtues of flexibility, simplicity, and physical transparency. It should be mentioned that a complete dynamic description of a nonequilibrium system should be based on two-time Green's functions, rather than a single-time density matrix. The former approach is too complex to be solved without substantial simplifying assumptions.[15] However, based on Dyson's equation, it provides more systematic approximation schemes. A detailed study of the relation between nonequilibrium Green's function approaches and the density matrix approach will be published elsewhere.[16]

Here, we apply the density matrix approach to a situation in which a subpicosecond laser pulse generates free electron-hole pairs of low to moderate densities in asymmetric GaAs-$Al_xGa_{1-x}As$ double wells. An external electric field is used to vary the relative position of the lowest electronic subbands associated with the two isolated wells. The peak energy and bandwidth of the laser are such that electron-hole pairs are created in the wide well, only, and such that the two lowest electronic subbands of the double well can be accessed. In our study, the typical pulse duration lies around 0.5 ps and the initial electron kinetic energy ranges from 12 to 20 meV. Hole subbands, which are involved in the excitation process, are far off resonance, so that hole tunneling between the two wells may be neglected and one may concentrate on electron motion. Holes are merely treated as a positive charge background to ensure that the total charge of the system remains zero. Due to the small initial excess energy per electron-hole pair, optical phonon emission, which generally plays an important role for carrier cooling on the pico- and subpicosecond time scale, is unimportant. The formation of excitons via LO phonon emission is neglected.

With these basic simplifying assumptions, one may reduce the problem to a study of the time evolution of an electronic one-particle density matrix,

$$\begin{pmatrix} f_{LL}(k,t)=\langle b^\dagger_{Lk}b_{Lk}\rangle(t) & f_{LR}(k,t)=\langle b^\dagger_{Lk}b_{Rk}\rangle(t) \\ f_{RL}(k,t)=\langle b^\dagger_{Rk}b_{Lk}\rangle(t) & f_{RR}(k,t)=\langle b^\dagger_{Rk}b_{Rk}\rangle(t) \end{pmatrix}, \tag{1}$$

where

$$\langle A\rangle = \mathrm{Tr}\{\rho A\}(t) \tag{2}$$

denotes the statistical average of an electron observable A over the full density operator ρ and b_α and $b^\dagger_\alpha$ are the single-particle operators for state α. The diagonal elements $f_{LL}(k,t)$ and $f_{RR}(k,t)$ are the electron distribution functions associated with left and right well, respectively, and k denotes the magnitude of the k-vector associated with in-plane motion. Inclusion of off-diagonal elements $f_{RL}(k,t)$ ("polarizations") allows a theoretical account of coherence in the system. The fact that one subband per quantum well is involved renders the density matrix a 2×2 matrix for given k. The spin degree of freedom is not accounted for in our notation, but is simply incorporated in the electron density of states. The basis states $|Lk\rangle$ and $|Rk\rangle$ are linear combinations of the two lowest eigenstates of the double well, $|+,k\rangle$ and $|-,k\rangle$ with eigenvalues $\epsilon_{+,k}$ and $\epsilon_{-,k}$, respectively. Here, $\epsilon_{\alpha,k}=\epsilon_\alpha+\frac{(\hbar k)^2}{2m^*}, \alpha=\pm,L,R$, assuming quasifree motion with effective mass m^* in the in-plane directions. The choice of a "left-right" basis $|L,k\rangle, |R,k\rangle$ is advantageous over the eigenkets $|+,k\rangle, |-,k\rangle$ of the double well in view of further simplifications that will be made below.

Structurally, perfect double wells are assumed throughout our calculations. Therefore, k is a good quantum number and the coupling between wells may be described by a single effective interwell coupling matrix element V. Different effective masses in well and barrier material give V a dependence on k. Due to the narrow energy regime, which is relevant here, this effect is ignored. The assumption of spatial uniformity parallel to the interfaces provides a major reduction in complexity of the problem, but may be somewhat unrealistic in real structures as structural imperfections may well provide a major source of dephasing in the system.[17]

The time-evolution of the density matrix is governed essentially by three physical processes. First, electron-hole pair generation by the light field changes the electron distribution functions. By suitable design of the double well and tuning of the properties of the laser pulse, carriers are initially generated in the wide well, only. Here, the carrier excitation process is accounted for by a Fermi-Golden-rule-type generation term,

$$\frac{d}{dt}f_{LL}(k,t)|_{\text{laser}} \tag{3}$$

with a Gaussian-shaped envelope of the pulse. As we are not concerned with ultrashort pulses (below 0.2 ps), high carrier densities, or the possibility of density fluctuations due to coherence induced additional generation and recombination processes,[10] this Markovian expression should be adequate for the present study.

Second, tunneling occurs between the left and right well, due to the fact that carriers are photoexcited into a coherent superposition of (approximately) symmetric and antisymmetric double-well states. The electronic structure is taken into account within a two-subband approximation for which the Hamiltonian reads,

$$H_0 = \sum_k \{\epsilon_{Lk} b^\dagger_{Lk} b_{Lk} + \epsilon_{Rk} b^\dagger_{Rk} b_{Rk} + V[b^\dagger_{Lk} b_{Rk} + b^\dagger_{Rk} b_{Lk}]\}. \quad (4)$$

H_o may be interpreted as the Hamilton operator of a system of (identical) noninteracting two-level systems, distinguished by their k vector, which are populated asymmetrically due to the action of the light field. In this structurally perfect system, no dephasing occurs due to H_0 and phase coherence is maintained even on a *macroscopic* level in the form of periodic charge oscillations. Based on H_0, such oscillations are induced if the duration of the laser pulse, which generates free electrons in the wide well, is small compared to the characteristic frequency of H_0. In other words, the phase relation between wave functions associated with different two-level systems is dictated by the creation process and remains unmodified under H_0. The time evolution of the density matrix under the influence of H_0 is fully coherent and reads

$$i\hbar \frac{d}{dt} f_{LL}(k,t)|_{H_0} = V[f^*_{RL}(k,t) - f_{RL}(k,t)] , \quad (5)$$

$$i\hbar \frac{d}{dt} f_{RR}(k,t)|_{H_0} = V[f_{RL}(k,t) - f^*_{RL}(k,t)] , \quad (6)$$

$$i\hbar \frac{d}{dt} f_{RL}(k,t)|_{H_0} = (\epsilon_{Lk} - \epsilon_{Rk}) f_{RL}(k,t) + V[f_{RR}(k,t) - f_{LL}(k,t)]. \quad (7)$$

Third, the appropriately screened (see Sec. II B below) Coulomb interaction between free electrons,

$$v = \frac{1}{2} \sum_{\alpha,\beta,\gamma,\delta,q,k,k'} v_{\alpha\beta\gamma\delta}(q) b^\dagger_{\alpha k+q} b^\dagger_{\beta k'-q} b_{\delta k'} b_{\gamma k}, \quad (8)$$

where $v_{\alpha\beta\gamma\delta}$, $\alpha, \beta, \gamma, \delta = L, R$, is the matrix element for the intercarrier Coulomb interaction, introduces a coupling between the two-level systems for each k.[18] Any initial phase coherence between electrons, which may have been established during the excitation process, decays as a consequence of this electron-electron interaction. As already known from similar studies of highly laser-excited bulk semiconductors, this first happens in second order in v, i.e., in its lowest-order scattering contribution.[10,19]

The Heisenberg equations of motion for $\langle b^\dagger_{ak} b_{a'k} \rangle$, $a, a' = L, R$ in the presence of the Coulomb interaction leads to the celebrated Bogoliubov-Born-Green-Kirkwood-Yvon (BBGKY) hierarchy, coupling the one-particle density matrix with all higher N-particle correlation functions.[20] Using $\tilde{b}$ for either $b^\dagger$ or b and dropping single particle labels, for brevity, this coupling is of the structure

$$\frac{d\langle \tilde{b}^2 \rangle}{dt} = O(\langle \tilde{b}^2 \rangle) + O(v\langle \tilde{b}^4 \rangle), \quad (9)$$

where $O(\,)$ indicates orders in v and $\tilde{b}$. The first term on the right-hand side (rhs) arises from H_0 and carrier generation due to the laser. The second term on the rhs arises from the Coulomb interaction. One is, in general, forced to find an approximation for this term. The simplest approach consists in self-consistent truncation procedures. Such a truncation may be performed at several levels. The simplest decomposition, which correctly accounts for terms up to order v on the rhs is of the structure $\langle \tilde{b}^4 \rangle(t) \approx \langle \tilde{b}^4 \rangle|_{\rm MF}(t) \propto O((\langle \tilde{b}^2 \rangle(t))^2)$ and leads to the mean-field (MF) approximation. For the Coulomb interaction, it merely leads to a (time-dependent) renormalization of the two–level parameters, which does not provide loss of phase coherence in the system. For the present study, which focuses on the damping aspect, one is thus forced to go at least one order higher and evaluate equations of motion of the general structure,

$$i\hbar \frac{d}{dt} \langle \tilde{b}^4 \rangle(t) = \langle [\tilde{b}^4, H] \rangle(t). \quad (10)$$

In the present basis, a significant reduction in complexity may be achieved if the right-hand side is replaced by $\langle [\tilde{b}^4, H(V = 0)] \rangle(t)$. This corresponds to neglecting *quantum*-interference terms between tunneling and the Coulomb interaction in the equations of motion.

The equations of motion then have the structure

$$i \frac{d}{dt} \langle \tilde{b}^4 \rangle(t) = \omega_4 \langle \tilde{b}^4 \rangle(t) + O(v\langle \tilde{b}^6 \rangle(t)), \quad (11)$$

with ω_4 equal to the sum of the negative (for each $b^\dagger$) and positive (for each b) free-particle energies associated with the respective $\tilde{b}^4$. The first term on the rhs arises from $H_0(V = 0)$, and the second term is due to the intercarrier Coulomb interaction. Truncation of the hierarchy can now be performed by manipulation of the integral expression in the exact solution to the initial-value problem,

$$\langle \tilde{b}^4 \rangle(t) = \langle \tilde{b}^4 \rangle(t)|_{H_0} - i \int_0^{t-t_0} dt' e^{-i\omega_4 t'} O(v\langle \tilde{b}^6 \rangle)(t - t'). \quad (12)$$

Within order v, one may retain the time evolution of $\langle \tilde{b}^6 \rangle$, with respect to H_0, i.e. that of frequency ω_6 (defined in an analogous way as ω_4 above), leading to

$$\langle \tilde{b}^4 \rangle(t) \approx \langle \tilde{b}^4 \rangle(t)|_{H_0} - iO(v\langle \tilde{b}^6 \rangle(t)) \int_0^{t-t_0} dt' e^{-i\omega' t'}, \quad (13)$$

with $\omega' = \omega_4 - \omega_6$. Second, in the integral on the rhs, one replaces ω' by $\omega' - i\eta$, with $\eta \to 0^+$, and takes $t_0 \to -\infty$. These two steps correspond to a phenomenological build in of dissipation ("memory loss") arising from unspecified interactions and/or higher-order terms, which eliminates the non-Markovian nature of the equation of motion. It ensures a causal response of the system. This gives

$$\langle \tilde{b}^4 \rangle(t) \approx \langle \tilde{b}^4 \rangle(t)|_{H_0} - \left[\mathcal{P} \frac{1}{\omega'} + i\pi\delta(\omega') \right] O(v\langle \tilde{b}^6 \rangle)(t). \quad (14)$$

In a third step, $\langle \tilde{b}^6 \rangle(t)$ is factorized into one-particle den-

sity matrix elements $\langle\tilde{b}^2\rangle(t)$, guided by Wick's theorem for noninteracting systems. This factorization leaves us with such combinations of state indices to yield $\omega' = \omega_4$ in equation (16). The resulting contribution to the time evolution of the densities recovers thereby the free-energy-conserving δ functions of semiclassical Boltzmann transport. Only terms of order $\langle\tilde{b}^2\rangle^2(t)$ need to be retained in our low density regime. Finally, renormalizing principal value terms $\mathcal{P}$ are neglected and $\langle\tilde{b}^4\rangle(t)|_{H_0}$ is approximated by its mean-field expression $\langle\tilde{b}^4\rangle(t)|_{\rm MF} \propto O([\langle\tilde{b}^2\rangle(t)]^2)$. Comparison with the Keldysh approach shows that this truncation procedure corresponds essentially to the screened Hartree-Fock approximation to the Coulomb self-energy.[16]

Two further assumptions were made in the derivation of the particle-particle interaction contribution used for this study. Exchange terms were neglected. While this can be rigorously justified in certain situations, such as a degenerate electron gas close to thermal equilibrium, this step here is made for simplicity. Finally, only $v_{\alpha\beta\alpha\beta}$ contributions are considered. This means that Coulomb scattering-induced tunneling is neglected. This effect should be insignificant as long as the overlap (V) between wave functions of different wells is small. Without this simplification, using $\{|+,k\rangle, |-,k\rangle\}$ for a basis set would be advantageous because, at the same level of complexity, Coulomb-tunneling quantum-interference terms can readily be included. However, this would lead to more complex connections between the densities in the left and right wells as the basic experimental "observables;" in particular, these quantities would contain polarization contributions. It should be added that the distinction between distribution functions and polarizations is solely based on the choice of the independent-particle basis. The latter, of course, is guided by the physical situation and characteristic observables of the system.

In summary, this procedure leads to an inclusion of the carrier-carrier interaction within the (screened) mean-field approximation,

$$\frac{d}{dt}f_{ab}(k,t)|_{\rm MF} = \frac{d}{dt}f_{ab}(k,t)|^{e-e}_{\rm MF} + \frac{d}{dt}f_{ab}(k,t)|^{e-h}_{\rm MF}$$

$$\begin{aligned}\frac{d}{dt}f_{ab}(k,t)|^{e-e}_{\rm MF} = &-\frac{i}{\hbar}f_{ab}(k,t)\sum_{\gamma}N_\gamma[v_{b\gamma b\gamma}(0) - v_{\gamma a\gamma a}(0)]\\ &-\frac{i}{\hbar}\sum_{\gamma,k'}[v_{\gamma a\gamma a}(|\vec{k}-\vec{k}'|)\\ &\times f_{\gamma b}(k,t)f_{a\gamma}(k',t)\\ &-v_{b\gamma b\gamma}(|\vec{k}-\vec{k}'|)f_{a\gamma}(k,t)f_{\gamma b}(k',t)]\end{aligned}$$

$$\frac{d}{dt}f_{aa}(k,t)|^{e-h}_{\rm MF} = 0$$

$$\begin{aligned}&\frac{d}{dt}f_{RL}(k,t)|^{e-h}_{MF}\\ &\quad = -\frac{i}{\hbar}(N_L + N_R)\,[v_{LLLL}(0) - v_{LRLR}(0)]f_{RL}(k,t),\end{aligned} \tag{15}$$

where N_γ is the total number of electrons in well γ, and within the scattering approximation,

$$\begin{aligned}\frac{d}{dt}f_{ab}(k,t)|_{\rm scat} &= \frac{d}{dt}\langle b^\dagger_{ak}b_{bk}\rangle|^{e-e}_{\rm scat}\\ &= \frac{\pi}{\hbar}\sum_{\gamma,q,k'}\delta\left(\frac{\hbar^2}{m^*}\vec{q}(\vec{k}-\vec{k}')\right)\{2v_{\gamma a\gamma a}(q)v_{\gamma b\gamma b}(q)f_{\gamma\gamma}(k',t)f_{ab}(|\vec{k}-\vec{q}|,t)\\ &\quad -[v_{\gamma a\gamma a}(q)^2 + v_{\gamma b\gamma b}(q)^2]f_{ab}(k,t)f_{\gamma\gamma}(|\vec{k}'-\vec{q}|,t)\}.\end{aligned} \tag{16}$$

The equation of motion of the system is a generalized Boltzmann equation in the density matrix elements and contains a tunneling contribution, a scattering contribution and an electron generation term. Owing to simplifications made above, quantum-interference terms between optical excitation, tunneling, and the Coulomb interaction are not accounted for. A clean inclusion of the latter would lead to a significant complication of matters, in particular, the simple scattering approximation (δ function in free-particle energies) would break down.

B. Free-carrier screening

Any assessment of the role of the electron-electron interaction in the dephasing and cooling process of the electron-hole system calls for a careful implementation of free-carrier screening. A clean implementation of screening in far-from-equilibrium situations is a highly complicated and rather controversial matter. For the present study, it is important not to underestimate the strength of the Coulomb interaction. Static screening, which is very appealing for its numerical simplicity, has been claimed to overestimate screening in non–equilibrium situations in 3D, although differences at densities below about 1×10^{16} cm^{-3} seem to be of minor importance.[11]

The Coulomb matrix elements $v_{\alpha\beta\gamma\delta}$ are evaluated for wave functions associated with infinitely deep wells. Consequently, we consider only matrix elements of the form $v_{\alpha\beta\alpha\beta}$. The unscreened Coulomb matrix elements are

$$\begin{aligned}v_{\alpha\alpha\alpha\alpha}(q) \equiv v_{\alpha\alpha}(q) \equiv v_c(q)\Bigg[&\frac{qL_\alpha}{(qL_\alpha)^2+(2\pi)^2} + \frac{2}{qL_\alpha}\\ &-2\left(\frac{(2\pi)^2}{qL_\alpha[(L_\alpha q)^2+(2\pi)^2]}\right)^2\\ &\times\left(1-e^{-qL_\alpha}\right)\Bigg]\end{aligned} \tag{17}$$

and

$$v_{\alpha\beta\alpha\beta}(q) = v_{\alpha\beta}(q) = v_c(q)e^{-qd}\frac{(1-e^{-L_\alpha q})(1-e^{-L_\beta q})}{L_\alpha L_\beta q^2} \times \frac{(2\pi)^4}{[(qL_\alpha)^2+(2\pi)^2][(qL_\beta)^2+(2\pi)^2]}, \tag{18}$$

where

$$v_c(q) = \frac{2\pi e^2}{\varepsilon_0 q}; \tag{19}$$

d is the barrier thickness, ε_0 the background dielectric constant, and L_α the width of well α. For qL_α, $qd \ll 1$, $v_{\alpha\alpha}(q) \approx v_{\alpha\beta}(q) \approx v_c(q)$. The second-order Coulomb singularities require implementation of free-carrier screening, corresponding to the well-established screened-Hartree-Fock approaches for the (equilibrium) electron gas. As our truncation procedure amounts to a termination of the BBGKY hierarchy at second order in v, screening has to be put in by hand. Our final result may be justified by a more complex truncation method or an alternative approach based on the Keldysh formalism.[16]

Screening for ultrafast carrier dynamics should be treated in the real time domain, rather than in the frequency domain using a single frequency. The latter version is only valid in steady-state situations, but questionable if significant modifications in the carrier distributions occur on the time scale which characterizes the particle-particle interactions, which may be the case during ultrafast laser excitation of carriers.[22] Moreover, the Coulomb interaction is a two-particle interaction and, thus, requires an inspection of the vertex function in the Bethe Salpeter equation,[23] rather than standard linear-response theory with respect to an external perturbation.

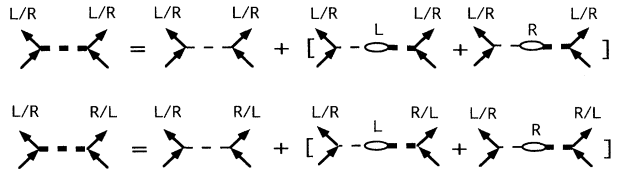

FIG. 1. Diagrammatic representation of screening in a two-component carrier system (left L, right R) within the random-phase approximation. Thick dashed line: screened Coulomb interaction; thin dashed line: bare Coulomb interaction.

Here, we adopt a commonly used shortcut and treat screening within the random-phase approximation (RPA). This corresponds to inserting electron-hole bubbles into the photon line of the bare vertex. A diagrammatic representation of the resulting Dyson-type equation for a two-component plasma is given in Fig. 1. Considering only two types of carriers, i.e., electrons in the left and right well, one obtains a simple 2×2 matrix problem, which gives the screened potentials,

$$v^{\mathrm{RPA}}_{\alpha\alpha}(q,\omega) = \frac{v_{\alpha\alpha}(q) + [v_{LR}(q)v_{RL}(q) - v_{LL}(q)v_{RR}(q)]D^0_\beta(q,\omega)}{[1-v_{LL}(q)D^0_L(q,\omega)][1-v_{RR}(q)D^0_R(q,\omega)] - v_{LR}(q)v_{RL}(q)D^0_L(q,\omega)D^0_R(q,\omega)}, \tag{20}$$

$$v^{\mathrm{RPA}}_{\alpha\beta}(q,\omega) = \frac{v_{\alpha\beta}(q)}{[1-v_{LL}(q)D^0_L(q,\omega)][1-v_{RR}(q)D^0_R(q,\omega)] - v_{LR}(q)v_{RL}(q)D^0_L(q,\omega)D^0_R(q,\omega)}, \tag{21}$$

$\alpha = L, R$, $\beta = R, L$, $\alpha \neq \beta$.

$$D^0_\alpha(q,\omega) = \frac{2}{(2\pi)^2}\int d^2k \frac{f_{\alpha\alpha}(k) - f_{\alpha\alpha}(|\mathbf{k}+\mathbf{q}|)}{\hbar\omega + \epsilon_\alpha(k) - \epsilon_\alpha(|\mathbf{k}+\mathbf{q}|) + i\eta}, \tag{22}$$

is the retarded density fluctuation correlation function for noninteracting carriers of type α, known as the Lindhard function. Thus, screening by free carriers in a two-component plasma is not strictly additive, in general. This is, however, the case for the analogous situation of bulk electron-hole systems, owing to $v_{\mathrm{ee}}(q) = v_{\mathrm{hh}}(q) = -v_{\mathrm{eh}}(q)$. Moreover, it can be seen that the screened interaction has acquired an ω dependence. This is an artifact of making a steady-state assumption, in which both the past and future of the system are known. Then it is easily verified that $\hbar\omega$ is equal to the energy, which is exchanged in the collision process to be screened.

For interactions, which favor small wave-vector exchange, the plasmon-pole approximation (PPA) offers a simple approximation to the density correlation function.[14] In 2D, it is of the form

$$D^0_\alpha(q,\omega) \approx D^{\mathrm{PPA}}_\alpha(q,\omega) = \frac{1}{v_c(q)}\frac{\omega^2_{\mathrm{pl}\alpha}(q)}{(\omega+i\eta)^2 - \frac{q}{\kappa_\alpha}\omega^2_{\mathrm{pl}\alpha}(q)}, \tag{23}$$

where $\omega^2_{\mathrm{pl}\alpha}(q) = (2\pi e^2 n_\alpha)/(\varepsilon_0 m^*)q$ is the square of the plasma frequency at sheet charge density n_α, $\kappa_\alpha = \frac{2}{a^*_B} f_{\alpha\alpha}(0)$ the $q \to 0$, i.e., the long-wavelength static (LWS RPA) screening wave vector in two dimensions, and a^*_B the effective Bohr radius. $D^{\mathrm{PPA}}_\alpha(q,\omega)$ is constructed in such a way that its $q \to 0$ limits for both $\omega = 0$ and $\omega \neq 0$ agree with those of the Lindhard expression. Setting $\hbar\omega$ equal to the energy transfer in the

collision, one obtains

$$\lim_{q\to 0} D_\alpha^{\mathrm{PPA}}\left(q,\omega=\frac{\hbar}{2m_\alpha^*}\mathbf{q}\cdot(\mathbf{q}-2\mathbf{k})\right) = -\varepsilon_0/(2\pi e^2)\frac{\kappa_\alpha}{1-[f_{\alpha\alpha}(0)/(\pi n_\alpha)]k^2\cos^2(\theta)} \tag{24}$$

for $\alpha = L, R$.

The general expression when $[f_{\alpha\alpha}(0)/(4\pi n_\alpha)](q - 2k\cos\theta)^2 \neq 1$ is

$$D_\alpha^{\mathrm{PPA}}\left(q,\omega=\frac{\hbar}{2m_\alpha^*}\mathbf{q}\cdot(\mathbf{q}-2\mathbf{k})\right) = -\varepsilon_0/(2\pi e^2)\frac{\kappa_\alpha}{1-[f_{\alpha\alpha}(0)/(4\pi n_\alpha)](q-2k\cos\theta)^2}, \tag{25}$$

for $\alpha = L, R$.

Here, θ is the angle between $\mathbf{k}$ and $\mathbf{q}$. In the limit $[f_{\alpha\alpha}(0)/(4\pi n_\alpha)](q - 2k\cos\theta)^2 \ll 1$, the PPA reduces to the LWS RPA expression. For a more detailed discussion of the PPA in the present case versus the 3D situation, we refer to Appendix A.

In the "static" screening approximation, ω is simply set equal to zero. If, in addition, the $q \to 0$ limit is taken, one obtains the above mentioned LWS RPA screening,[21]

$$\lim_{q\to 0} D_\alpha^0(q,0) = -\frac{m_\alpha^*}{\hbar^2\pi} f_{\alpha\alpha}(0). \tag{26}$$

Equation (26) is not based on the assumption of thermal equilibrium. The classical Debye-Hückel (DH) method, applicable to a nondegenerate electron gas in thermal equilibrium, gives

$$\lim_{q\to 0} D_\alpha^{\mathrm{DH}}(q,0) = -\frac{3n_\alpha}{2\langle E\rangle_\alpha}, \tag{27}$$

where $\langle E\rangle$ is the average kinetic energy of an electron in well $\alpha = L, R$. Note that PPA and LWS RPA approximations give an explicit dependence on the band edge occupation $f_{\alpha\alpha}(0)$, while the DH approximation gives an explicit dependence on average particle energy and total number of particles. This has a certain influence on the buildup of screening within the different approximations and will be discussed below.

III. NUMERICAL RESULTS AND DISCUSSION

We have performed a systematic series of numerical calculations to investigate whether short-pulse laser generation of free charge carriers can induce coherent charge oscillations in structurally perfect asymmetric semiconductor double wells. Calculations were performed for two GaAs-$Al_xGa_{1-x}As$ double wells under various excitation conditions. Structure A is a $GaAs/Ga_{0.65}Al_{0.35}As$ double well with a 17 Å barrier separating 170 Å and 120 Å wells, corresponding to an interwell coupling $V \approx -1.5$ meV. Structure B is a $GaAs/Ga_{0.80}Al_{0.20}As$ double well with a 25 Å barrier separating 150 Å and 100 Å wells, corresponding to an interwell coupling $V \approx -2.5$ meV.

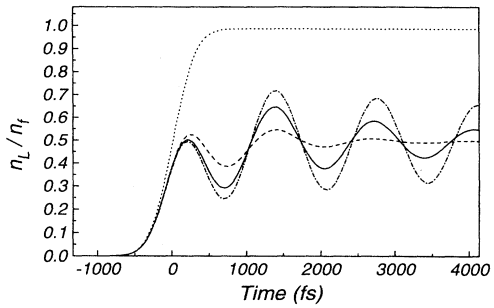

FIG. 2. Normalized electron density in the left (wide) well as a function of time for structure A. Final electron densities n_f are 0.3×10^{10} cm^{-2} (dot-dashed line), 1.0×10^{10} cm^{-2} (solid line), and 3.0×10^{10} cm^{-2} (dashed line). The dotted line gives the total normalized electron density. The laser excess energy is 20 meV and the screening model is the LWS RPA.

A. Carrier dynamics

A typical set of numerical results is displayed in Figs. 2–9. The light field was given a Gaussian spectral profile with a width of 4.2 meV, a duration of 0.5 ps, and provided an average initial kinetic energy of 20 meV per excited electron. Figures 2–4 and 5–7, respectively, were obtained for structures A and B at resonance bias. In all cases, time zero coincides with the peak of the laser pulse. Figures 2 and 5 display the normalized total electron density in the left (wide) well as a function of time for final electron densities n_f of 0.3×10^{10} cm^{-2} (dot-dashed line), 1.0×10^{10} cm^{-2} (solid line), and 3.0×10^{10} cm^{-2} (dashed line). Figures 3 and 6 give the equivalent information for the right (narrow) well, whereas Figs. 4 and 7 give the normalized total polarization as a function of time. LWS RPA screening was used to obtain these

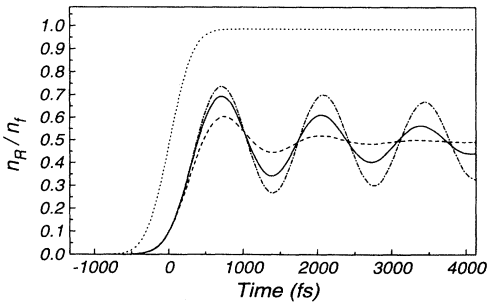

FIG. 3. Normalized electron density in the right (narrow) well as a function of time for structure A. Other parameters as stated in Fig. 2.

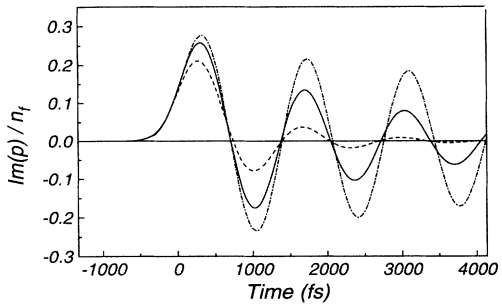

FIG. 4. Normalized total polarization as a function of time for structure A. Other parameters as stated in Fig. 2.

data. In this density regime, damped charge oscillations are obtained in all cases. At low electron densities, they are more pronounced in structure A, due to a larger ratio between tunneling period and pulse duration. The same holds for the total polarization in Figs. 4 and 7. For both A and B, the largest amplitude of the oscillations occurs in the narrow well, rather than the wide well, in which carriers are excited originally. This is a consequence of the finite pulse duration, tunneling, and damping. Simple interpolation to shorter pulses predicts an increase of the amplitude of the oscillations, with decreasing pulse duration.

The damping of the coherent charge oscillations is accompanied by a gradual thermalization of electrons, which occurs on roughly the same time scale. The electron distribution $f_{\rm tot}(k) = f_{LL}(k) + f_{RR}(k)$ is plotted in Figs. 8 and 9, for structure A and B, respectively, for six different times and a final electron density $n_f = 1 \times 10^{10}$ cm^{-2}. In the long-time limit and at resonance bias the normalized electron densities per well approach the value one half, while polarizations decay to zero. Other runs performed at lower initial kinetic excess energy gave very similar results. Figure 10 shows a comparison between 12 meV and 20 meV excess energy for structure A and $n_f = 1 \times 10^{10}$ cm^{-2}. Just as the thermalization process takes somewhat longer at higher excitation energies, so does the damping of the charge oscillations.

Under present excitation conditions, the critical density at which the transition from weak to strong damping occurs is about 1.0×10^{10} cm^{-2}. At these electron densities, MF-renormalization effects are still negligible for the time evolution of the system. In Figs. 2–7, this is apparent from the density independence of the oscillation frequency. Numerical results which include MF corrections are indistinguishable from those which omit MF corrections when plotted in figures, such as Figs. 2–7. Damping, on the other hand, is a sensitive function of the electron density in both structures. Below 1.0×10^9 cm^{-2} damping is very weak, while oscillations are suppressed above about 5.0×10^{10} cm^{-2}. We have fitted the time evolution of electrons in the wide well of the structures for *instantaneous* generation of all carriers, using the ansatz $n_L(t) = (n_f/2)\ [1 + \exp(-t/\tau)\ \cos(\omega_0 t)]$, where $1/\tau$ is a phenomenological damping constant fitted to our numerical results. $(2\pi\tau)/\omega_0$ is plotted versus n_f in Fig. 11. It displays a strong dependence on the electron density, but is virtually identical for structure A (diamonds) and B (circles).

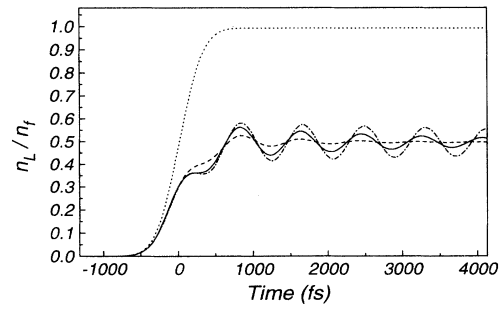

FIG. 5. Normalized electron density in the left (wide) well as a function of time for structure B. Other parameters as stated in Fig. 2.

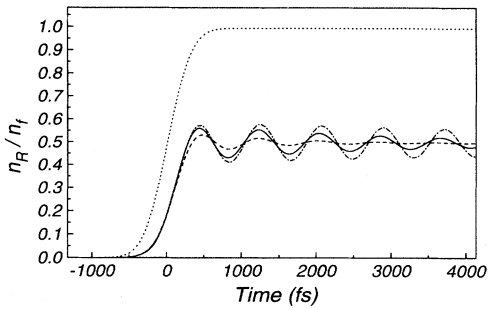

FIG. 6. Normalized electron density in the right (narrow) well as a function of time for structure B. Other parameters as stated in Fig. 2.

B. Free-carrier screening

According to Sec. II B, several models were used for free-carrier screening of the electron-electron Coulomb interaction. We compared the results obtained within different screening models, in particular, static screening models to dynamic screening within the PPA. For all den-

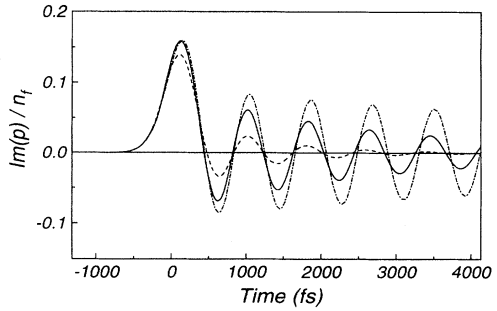

FIG. 7. Normalized total polarization as a function of time for structure B. Other parameters as stated in Fig. 2.

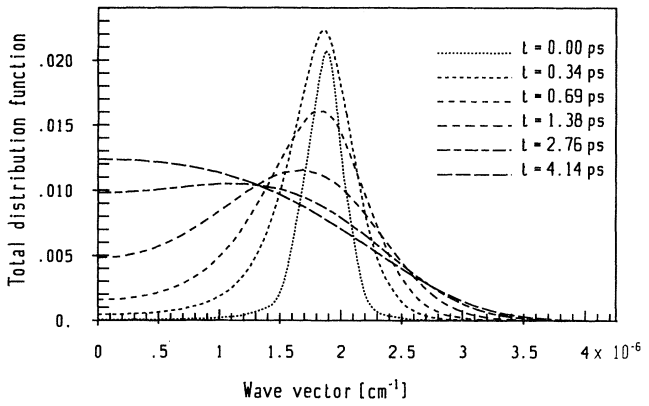

FIG. 8. Total electron distribution function $f_{\rm tot}(k) = f_{LL}(k) + f_{RR}(k)$ for structure A at selected times. Excitation conditions are as in Fig. 2 for the case of $n_f = 1.0 \times 10^{10}$ cm^{-2}.

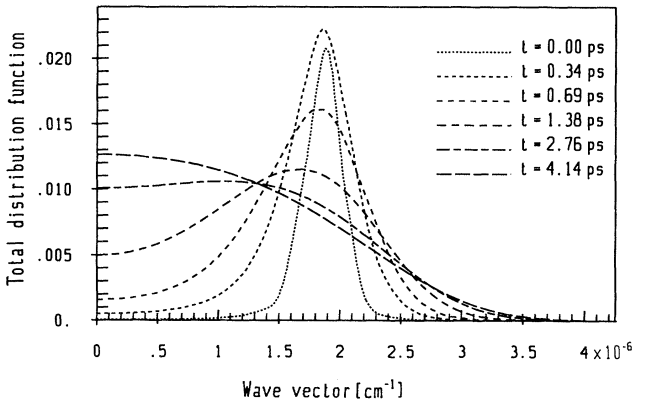

FIG. 9. Total electron distribution function $f_{\rm tot}(k) = f_{LL}(k) + f_{RR}(k)$ for structure B at selected times and excitation conditions as in Figs. 2 for the case of $n_f = 1.0 \times 10^{10}$ cm^{-2}.

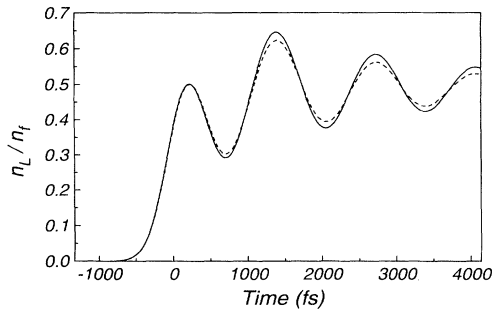

FIG. 10. Normalized electron density in the left (wide) well as a function of time for structure A. Final electron density n_f is 1.0×10^{10} cm^{-2}, laser excess energies are 20 meV (solid line) and 12 meV (dashed line). The screening model is the LWS RPA.

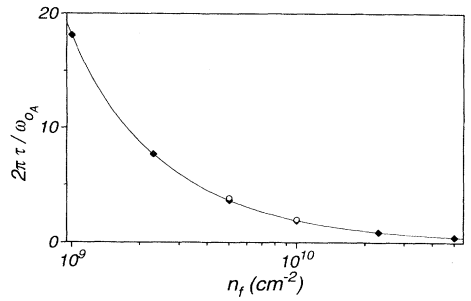

FIG. 11. Normalized damping time versus final electron density for instantaneous electron generation. Structure A: diamonds; structure B: circles. The excess energy is 20 meV, the screening model is DH.

sities at which charge density oscillations were obtained in our calculations, the screening model turned out to be rather immaterial, although some form of screening was necessary to avoid the singularity of the Coulomb potential at $q = 0$. Within the accuracy of our figures, the dynamics of the system was not affected by the particular screening version which was adopted. In particular, no differences of any significance were found in the dynamics of the system when dynamic screening within the PPA was used instead of LWS RPA screening. DH screening provided somewhat stronger screening than LWS RPA screening and the PPA. A comparison between the screening wave vector within DH versus that within LWS RPA is given in Fig. 12. The different behavior is due to the fact that DH is an equilibrium screening model, which relates the screening wave vector to the carrier density, whereas LWS RPA may also be valid for nonequilibrium carrier distributions. In the present case, DH predicts stronger screening than LWS RPA. The buildup of DH screening is dictated by the carrier generation rate only, while, for the LWS RPA, it is primarily governed by the thermalization dynamics.

As discussed in the Appendix, dynamic screening within the PPA does not modify the results obtained within the LWS RPA, because the plasmon-pole contribution is negligible for relevant k vectors and time scales. On the time scale where it is decided whether charge oscillations may form, $[f_{\alpha\alpha}(0)/(4\pi n_\alpha)][q - 2\cos(\theta)k]^2 \ll 1$.

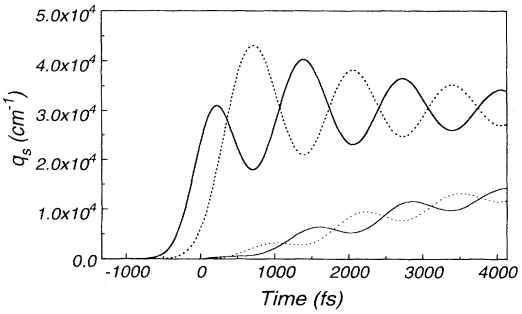

FIG. 12. Screening wave vectors within DH (thick lines) and LWS RPA (thin lines) for left (solid lines) and right well (dashed lines). Final electron density is 1.0×10^{10} cm^{-2}, laser excess energy is 20 meV.

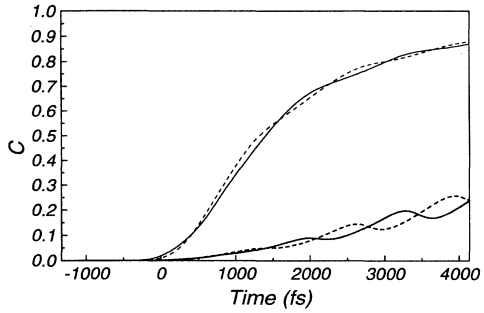

FIG. 13. $C_\alpha \equiv f_{\alpha\alpha}(0)\langle k^2\rangle/(2\pi n_\alpha)$, $\alpha = L$ (solid lines), $\alpha = R$ (dashed lines), versus time for structure A. Final electron densities are $n_f = 0.3 \times 10^{10}$ cm^{-2} (lower lines) and $n_f = 3 \times 10^{10}$ cm^{-2} (upper lines). Laser excess energy is 20 meV.

The quantity $[f_{\alpha\alpha}(0)/(2\pi n_\alpha)]\langle k\rangle^2$, corresponding to $q = 0$ and scattering at the average carrier energy, is plotted as a function of time in Fig. 13 for the same parameters as in Figs. 2–4 and a final carrier concentration of 1.0×10^{10} cm^{-2}. As long as this quantity remains less than one, the plasmon pole is ineffective and leaves the PPA virtually identical to LWS RPA. At low carrier concentrations and initial carrier generation above the band edge, the carrier thermalization process, which leads to a population of the band edge is too slow to influence the onset of the oscillations. As our results are independent of the screening model used, we are rather confident that we have provided a satisfactory picture of this aspect of the electron-electron interaction in the double well for a pulse duration around 0.5 ps and electron densities below 5×10^{10} cm^{-2}.

IV. SUMMARY AND CONCLUSIONS

In summary, we have conducted a theoretical study of the dynamics of photogenerated electrons in resonance-biased asymmetric double wells. Our main objective was to determine the role played by the electron-electron Coulomb interaction in damping or suppressing coherent free charge oscillations induced by selective subpicosecond electron-hole pair generation in the wide well. Our calculations are based on the density matrix approach, which was developed for an interacting electron-hole system in a double well. Whereas the electron-hole interaction was treated within the mean-field approximation, the scattering approximation was used to account for the electron-electron Coulomb interaction.

For structures which are typical for the investigation of exciton-related oscillations, we find that charge oscillations due to free electron tunneling between the wide and narrow well are permitted for electron densities of up to about 5×10^{10} cm^{-2}, in spite of the phase-destroying role played by the Coulomb interaction. This result is virtually independent from the screening models that we used to account for free-carrier screening, i.e., Debye-Hückel, long-wavelength static RPA, and Lindhard within the PPA. No noticeable difference was found between dynamic and static screening. While renormalization was found to be negligible at relevant carrier densities, the rate of dephasing caused by the Coulomb interaction was found to be strongly density dependent.

It should be emphasized that the present study ignores the possibility of dephasing processes caused by structural imperfections. It is clear that the latter will dominate at sufficiently low carrier concentrations. Samples of high structural uniformity are mandatory if the electron-electron Coulomb interaction is to provide the main mechanism to damp or suppress charge density oscillations.

At present, there seems to be no experimental evidence for the existence of coherent free-carrier charge oscillations in double wells. It is not clear at present, whether this is due to difficulties in observing their presence, the dominance of other dephasing mechanisms, and/or an underestimation of the strength of the Coulomb interaction in the (initial) stages of the time-evolution. Recent experiments in bulk, which indicate the occurrence of coherent free charge oscillations in an applied linear electric field seem to point towards the first possibility.[9] However, a critical assessment of our present approximations is called for in any case. We adopted a Markovian source term to account for generation of free carriers, with time-energy uncertainty put in by hand. It is valid as long as the pulse duration is larger than approximately 0.1 ps and charge densities are low. Similarly, standard dynamic screening should still be reasonably accurate on the present time scale, as discussed in detail. The electron-hole interaction beyond the simple mean-field interaction has been neglected. This could modify our results somewhat. However, it is known that the electron-hole interaction is less effective in the cooling process than the electron-electron and hole-hole interaction. The degree of inelasticity is frequently thought to influence dephasing, with higher inelasticity leading to more rapid dephasing.[24,25] This trend is, in fact, confirmed by a discussion of the validity of the approximations which lead from Eq. (12) to Eq. (14). In the worst case, we expect a factor of two in the damping constant. Interference terms between laser excitation, Coulomb scattering, and tunneling have been neglected. It is difficult to quantitatively estimate the importance of these terms in the equations of motion, because the computational tractability of the theory largely rests upon this simplification. Finally, the carrier-phonon interaction has been neglected as a possible source for dephasing. This is justified by low initial excess energies and the time scale on which the charge oscillations build up. Nevertheless, further improvements to our approach are desirable. More realistic wave functions than those associated with infinitely deep wells should be used. Consequently, the influence of Coulomb-induced tunneling and the effect of an effective mass discontinuity at the heterointerfaces should be investigated. Finally, holes should be treated on equal footing with electrons.

ACKNOWLEDGMENT

W.P. acknowledges support from the US Army Research Office.

APPENDIX: PLASMON-POLE APPROXIMATION VERSUS STATIC SCREENING

The purpose of this appendix is to discuss static screening versus dynamic screening within the PPA. The PPA replaces the complicated pole structure of the retarded density fluctuation correlation function for a noninteracting gas of carriers by[14]

$$D^{\mathrm{PPA}}(q,\omega)=\frac{1}{v_c(q)}\frac{\omega_{\mathrm{pl}}^2(q)}{(\omega+i\eta)^2-\frac{q}{\kappa}\omega_{\mathrm{pl}}^2(q)}, \tag{A1}$$

in two spatial dimensions, and

$$D^{\mathrm{PPA}}(q,\omega)=\frac{1}{V_c(q)}\frac{\Omega_{\mathrm{pl}}^2}{(\omega+i\eta)^2-\frac{q^2}{\tilde{\kappa}^2}\Omega_{\mathrm{pl}}^2}, \tag{A2}$$

with $V_c(q)=4\pi e^2/(\epsilon_0 q^2)$, $\Omega_{\mathrm{pl}}^2=4\pi e^2 n/(\epsilon_0 m^*)$, in three spatial dimensions. The corresponding 2D expressions are defined in Sec. II B. The specific form of the screening wave vectors κ and $\tilde{\kappa}$, in general, depends on assumptions made upon the carrier distribution functions. Both expressions imply the limit $\eta\to 0_+$. For screening of the matrix elements in the density matrix equations, one sets $\omega=\frac{\hbar}{2m^*}q(q-2k\cos\theta)$, where k is the magnitude of the wave vector associated with either the initial or final one-particle state and θ is the angle between $\mathbf{q}$ and $\mathbf{k}$.

To begin with the 2D case, consider first the special case $q=2k\cos\theta$. This corresponds to zero energy exchange, in which case PPA and long-wavelength static RPA (LWS RPA) screening are equivalent. Now consider the general case, but for $q\neq 2k\cos\theta$. One may write

$$D^{\mathrm{PPA}}(q,\omega)=\frac{a/(2bcq-2k\cos\theta)}{(cq-2k\cos\theta)/2-a/(2c\kappa q-2k\cos\theta)+i\eta}, \tag{A3}$$

where a,b,c are constants. In particular, $\omega_{\mathrm{pl}}^2(q)=aq$, $v_c(q)=b/q$, and $c=\hbar/(2m^*)$. A pole arises when

$$\frac{(q-2k\cos\theta)^2 f(0)}{4\pi n}=1. \tag{A4}$$

To consider the relevance of the pole, first consider a system in thermal equilibrium at $T=0$ K. In this case,

$$\frac{(q-2k\cos\theta)^2 f(0)}{4\pi n}=\frac{(q-2k\cos\theta)^2}{2(k_F)^2}, \tag{A5}$$

where k_F is the Fermi wave vector. For a nondegenerate system at temperature T, one finds

$$\frac{(q-2k\cos\theta)^2 f(0)}{4\pi n}=\frac{\hbar^2(q-2k\cos\theta)^2}{4m^*k_BT}, \tag{A6}$$

where k_B is the Boltzmann constant. In both cases, for a typical collision process, this ratio will indeed be close to order one. Therefore, the PPA expression differs from the static result and a more detailed numerical investigation is called for to compare predictions within static and dynamic screening. Now consider the case of carrier generation by a subpicosecond laser pulse into the band at rather well-defined energy. During excitation and the initial stage of the cooling process, the ratio on the left-hand side is small for all wave vectors of interest, because only a small fraction of carriers populates the band edge. This means that the plasmon pole contributes little in the initial stage of events, i.e., during the subpicosecond excitation pulse and initial cooling of carriers. Therefore, only the real part of $D^{\mathrm{PPA}}(q,\omega)$ is relevant and one may write

$$D^{\mathrm{PPA}}(q,\omega)\approx-\frac{\kappa}{b}\frac{1}{1-\frac{f(0)}{4\pi n}(q-2k\cos\theta)^2}. \tag{A7}$$

It can be seen that, in 2D, the PPA for the screening of the Coulomb interaction is close to the LWS RPA, as long as the band edge occupation probability is sufficiently small compared to the total number of carriers present in the system. This condition is indeed fulfilled in the present situation, as was discussed in Sec. III B. In the present calculations, static and dynamic screening yield practically identical results. Only when thermalization progresses and the band edge becomes populated, does the plasmon pole move into the relevant region of q and k values.

The situation is somewhat different in 3D. First, the plasma frequency is q independent. More importantly, the screening wave vector for the long-wavelength limit is of the form $\tilde{\kappa}^2=2\pi e^2 n\langle 1/E\rangle/\epsilon_0$, where $\langle\rangle$ denotes the average over the normalized single-particle distribution function and n is the 3D particle density. Again, validity of the latter expression is not limited to thermal equilibrium. A similar analysis as above shows that the plasmon pole occurs when

$$\frac{\hbar^2(q-2k\cos\theta)^2}{8m^*}\left\langle\frac{1}{E}\right\rangle=1, \tag{A8}$$

a condition which is equally well met in and out of thermal equilibrium. In case of a Maxwellian distribution, resulting in the Debye-Hückel form for the screening length, $\tilde{\kappa}^2=\frac{4\pi e^2 n}{\epsilon_0 k_B T}$, one obtains the condition

$$\frac{1}{2}\frac{\hbar^2(q-2k\cos\theta)^2}{2m^*k_BT}=1. \tag{A9}$$

Thus, both real and imaginary part of $D^{\mathrm{PPA}}(q,\omega)$ need to be considered and dynamic screening within the PPA

may produce different results than static screening. Alternatively, consider a nonequilibrium distribution function $f(k)$, which is sharply peaked around k_0. Most $q \approx 0$ Coulomb scattering processes occur between states around k_0 and, again, the plasmon pole in Eq. (A2) will contribute. However, numerical studies have shown that the difference between the PPA and static screening is negligible at low carrier concentrations.[11]

[1] E. O. Göbel, Adv. Solid State Phys. **30**, 269 (1989); E. O. Göbel, K. Leo, T. C. Damen, J. Shah, S. Schmitt-Rink, W. Schäfer, J. F. Müller, and K. Köhler, Phys. Rev. Lett. **64**, 1801 (1990).

[2] P. C. Becker, H. L. Fragnito, C. H. Brito Cruz, R. L. Fork, J. E. Cunningham, J. E. Henry, and J. Shah, Phys. Rev. Lett. **61**, 1647 (1988).

[3] K. Leo, J. Shah, E. O. Göbel, T. C. Damen, S. Schmitt-Rink, W. Schäfer, and K. Köhler, Phys. Rev. Lett. **66**, 201 (1991).

[4] H. G. Roskos, M. C. Nuss, J. Shah, K. Leo, D. A. B. Miller, A. M. Fox, S. Schmitt-Rink, and K. Köhler, Phys. Rev. Lett. **68**, 2216 (1992).

[5] M. S. C. Luo, S. L. Chuang, P. C. M. Planken, I. Brener, and M. C. Nuss, Phys. Rev. B **48**, 11 043 (1993).

[6] C. Waschke, H. G. Roskos, R. Schwedler, K. Leo, H. Kurz, and K. Köhler, Phys. Rev. Lett. **70**, 3319 (1993).

[7] I. Brener, P. C. M. Planken, M. C. Nuss, M. S. C. Luo, S. L. Chuang, L. Pfeiffer, D. E. Leaird, and A. M. Weiner, J. Opt. Soc. Am. B **11**, 2457 (1994).

[8] D. S. Kim, J. Shah, J. E. Cunningham, T. C. Damen, W. Schäfer, M. Hartmann, and S. Schmitt-Rink, Phys. Rev. Lett. **68**, 1006 (1992).

[9] W. Sha, A. L. Smirl, and W. F. Tseng (unpublished).

[10] T. Kuhn and F. Rossi, Phys. Rev. B **46**, 7496 (1992).

[11] For a recent discussion in 3D, see, J. Collet, Phys. Rev. B **47**, 10 279 (1993).

[12] J. F. Young, T. Gong, P. M. Fauchet, and P. J. Kelly, Phys. Rev. B **50**, 2208 (1994).

[13] C. P. Slichter, *Principles of Magnetic Resonance*, 3rd ed. (Springer, Berlin, 1992).

[14] H. Haug and S. Koch, *Quantum Theory of the Optical and Electronic Properties of Semiconductors*, 2nd ed. (World Scientific, Singapore, 1993).

[15] A. V. Kuznetsov, Phys. Rev. B **44**, 8729 (1991).

[16] U. Hohenester and W. Pötz (unpublished).

[17] A. P. Heberle, W. W. Rühle, and K. Köhler, Phys. Status Solidi B **173**, 381 (1992).

[18] M. Žiger, W. Pötz, and P. Kocevar, SPIE Proc. **2142**, 87 (1994); M. Žiger and W. Pötz (unpublished).

[19] M. Lindberg and S. W. Koch, Phys. Rev. B **38**, 3342 (1988).

[20] R. Balescu, *Equilibrium and Nonequilibrium Statistical Mechanics* (Wiley-Interscience, New York, 1975).

[21] F. Stern, Phys. Rev. Lett. **18**, 546 (1967).

[22] K. El Sayed, S. Schuster, H. Haug, F. Herzel, and K. Henneberger, Phys. Rev. B **49**, 7337 (1994).

[23] S. Schmitt-Rink, D. B. Tran Thoai, and H. Haug, Z. Phys. B **39**, 25 (1980).

[24] See, for example, Y. Imry, in *Nanostructures and Mesoscopic Systems*, edited by W. P. Kirk and M. A. Reed (Academic Press, San Diego, 1992), pp. 11–23.

[25] T. Kuhn (private communication).